Published in final edited form as:

J Comp Neurol. 1999 June 07; 408(3): 419–436. doi:10.1002/(sici)1096-9861(19990607)408:3<419::aid-cne8>3.0.co;2-4.

Brainstem Projections to the Ventromedial Medulla in Cat: Retrograde Transport Horseradish Peroxidase and Immunohistochemical Studies

Y.Y. LAI[1,*], **J.R. CLEMENTS**[2], **X.Y. WU**[2], **T. SHALITA**[1], **J.-P. WU**[3], **J.S. KUO**[3], **J.M. SIEGEL**[1]

[1]Department of Psychiatry, School of Medicine, University of California, Los Angeles, and Neurobiology Research, VAMC, North Hills, California 91343

[2]Department of Veterinary Anatomy, Texas A&M University, College Station, Texas 77843

[3]Department of Medical Research, Taichung Veterans General Hospital, Taiwan, Republic of China

Abstract

Stimulation of the nucleus magnocellularis (NMC) of the medulla produces changes in locomotion, muscle tone, heart rate, and blood pressure. Glutamatergic input has been found to modulate muscle tone, whereas cholinergic input has been found to mediate cardiovascular changes produced by stimulation of the NMC. The current study was designed to identify the brainstem afferents to NMC by using retrograde transport of wheat germ agglutinin and horseradish peroxidase (WGA-HRP) combined with glutamate and choline acetyltransferase (ChAT) immunohistochemical and nicotinamide adenine dinucleotide phosphate-diaphorase (NADPH-d) histochemical techniques. Fifty nanoliters of 2.5% WGA-HRP were microinjected into the NMC in the cat. A heavy density of WGA-HRP-labeled neurons was found in the ipsilateral mesencephalic reticular formation (MRF), periaqueductal gray, Kolliker-Fuse nucleus, and pontis centralis caudalis (PoC), in the contralateral pontis centralis oralis (PoO), and bilaterally in the nucleus paragigantocellularis lateralis. A moderate density of retrogradely labeled neurons was found in the ipsilateral side of the nuclei parvocellularis, retrorubral (RRN), PoO, and vestibular complex, in the contralateral PoC and nucleus gigantocellularis, and bilaterally in the inferior vestibular nucleus. Retrograde HRP/glutamate-positive cells could be found throughout the brainstem, with a high percentage in RRN, PoO, PoC, and MRF. Double-labeled WGA-HRP/ChAT neurons were found in the pedunculopontine nucleus. Double-labeled WGA-HRP/NADPH-d-positive neurons could be seen in many nuclei of the brainstem, although the number of labeled neurons was small. The dense glutamatergic projections to the NMC support the hypothesis that rostral brainstem glutamatergic mechanisms regulate muscle activity and locomotor coordination via the NMC, whereas the pontine cholinergic projections to the NMC participate in cardiovascular regulation.

[*]Correspondence to: Y.Y. Lai, Ph.D., Neurobiology Research (151A3), VA Medical Center, 16111 Plummer Street, North Hills, CA91343.

Indexing terms:

choline acetyltransferase; NADPH; sleep apnea; cardiovascular; locomotion; REM sleep

Neurons in the nucleus magnocellularis (NMC) of the rostral ventromedial medulla have been shown to relate to electroencephalographic desynchronization (Moruzzi and Magoun, 1949), muscle atonia in rapid-eye-movement (REM) sleep (Siegel et al., 1979; Sakai et al., 1981), muscle tone suppression (Lai et al., 1987; Hajnik et al., 1995), and locomotion (Noga et al., 1988; Atsuta et al., 1990; Perreault et al., 1993). By using the decerebrate cat model, we found that microinjection of non-N-methyl-D-aspartate (non-NMDA) agonists and corticotropin-releasing factor (CRF) in NMC induces muscle atonia, whereas NMDA agonists induce muscle tone facilitation or locomotion (Lai and Siegel, 1988, 1991, 1992). Administration of NMDA into the nucleus gigantocellularis and ventralis of the rodent, corresponding to the NMC in the cat, also induces muscle tone facilitation and/or locomotion (Kinjo et al., 1990). However, cholinergic agonists microinjected into the same sites in the NMC produce cardiovascular changes (Lai and Siegel, 1990) but no changes in muscle activity (Lai and Siegel, 1988).

Neurons in the NMC project to the spinal cord (Tohyama et al., 1979; Newman, 1985). By using the microinjection technique, we found that glutamate antagonists injected into the NMC block pontine carbachol-induced muscle atonia in the decerebrate cat (Lai and Siegel, 1988), indicating that the output of the cholinoceptive pontis centralis oralis (PoO) mechanism responsible for the suppression of muscle tone is mediated by a glutamatergic descending pathway to the NMC. Non-NMDA agonists and NMDA antagonists microinjected into the NMC have been shown to attenuate or block muscle twitches in the decerebrate cat (Lai and Siegel, 1997b). The sources of glutamatergic afferent projection to this region remain unknown.

Nitric oxide (NO) synthase is present in many of the cholinergic neurons of the pontine brainstem and is identical to nicotinamide adenine dinucleotide phosphate-diaphorase (NADPH-d) in neurons (Vincent et al., 1983; Dawson et al., 1991). Inhibition of pontine NO synthase disrupts REM sleep and reduces pontine acetylcholine release (Datta et al., 1997; Leonard and Lydic, 1997). Intracerebroventricular administration of the NO synthase inhibitor 7-nitro indazole has marked effects on muscle tone and posture (Dzulfic et al., 1996). Systemic injection of the NO synthase inhibitor N-omega-nitro-L-arginine (Kapas et al., 1994a,b) and 7-nitro indazole (Dzoljic et al., 1996, 1997) suppresses sleep in the rabbit and rat, whereas administration of NO, S-nitroso-N-acetylpenicillamine, or molsidomine increases slow wave sleep in the rat (Kapas and Krueger, 1996).

The current experiment identified the projections of glutamate-, acetylcholine-, and NO synthase-containing neurons to the NMC by using retrograde transport of wheat germ agglutinated horseradish peroxidase (WGA-HRP) combined with glutamate and choline acetyltransferase (ChAT) immunocytochemical and NADPH-d histochemical techniques.

MATERIALS AND METHODS

All procedures were approved by the Animal Studies Committee of the Sepulveda VA Medical Center/UCLA in accordance with U.S. Public Health Service guidelines. Three male and four female adult cats weighing 2.0–4.1 kg served as subjects. Under sodium pentobarbital (Nembutal, 35 mg/kg, i.p.) anesthesia, a 1-μl Hamilton (7001-N) 25 sG syringe, angled at 15° in the sagittal plane to avoid the bony tentorium, was lowered to the NMC. Fifty nanoliters of 2.5% WGA-HRP were injected over a 5-minute period, and the needle was retained in place for an additional 15 minutes to minimize leakage up the needle track. All seven cats received a single unilateral injection into the NMC. After 2 days, the cats were deeply anesthetized with an overdose of Nembutal (50 mg/kg, i.p.) and perfused intracardially with 0.1 M phosphate buffered saline (PBS; pH 7.4) followed by cold (4°C) 3% paraformaldehyde and 0.25% glutaraldehyde in 0.1 M phosphate buffer (PB; pH 7.4). The brain tissues were removed and fixed in 3% paraformaldehyde in 0.1 M PBS, pH 7.4, for 2 hours at 4°C. Tissues were then transferred to 30% sucrose in 0.1 M PBS at pH 7.4.

Serial coronal sections were cut at 50 μ. Interdigitated series of sections from five cats (HM11, HM12, HM15, HM21, and HM22) were stained for NADPH-d, glutamate, WGA-HRP, NADPH-d and WGA-HRP, and glutamate and WGA-HRP. Alternate sections from the other two cats (HM13 and HM14) were stained for WGA-HRP, ChAT, and WGA-HRP and ChAT.

Our protocol for WGA-HRP combined with NADPH-d histochemical staining has been described previously (Lai et al., 1993). The method for NADPH-d staining was modified from that of Scherer-Singler et al. (1983). Immediately after cutting, sections were processed with a solution containing 15 mM of sodium malate, 1 mM NADPH, and 20 mM of nitro blue tetrazolium in 0.1 M Tris-HCl (pH8.0) for 15–30 minutes at 37°C. Sections were then rinsed with Tris buffer.

Neurons containing retrograde WGA-HRP label were identified by using tetramethylbenzidine (TMB; Mesulam, 1978). The blue crystalline TMB product was stabilized with a solution containing 0.05% diaminobenzidine (DAB), 0.02% cobalt chloride, and 0.02% hydrogen peroxide (Rye et al., 1984).

For identification of glutamatergic projections, sections were rinsed with 0.1 M PB and then incubated with normal goat serum. Subsequently, sections were incubated with polyclonal antibody raised in rabbit against glutamate (Arnel Products, New York, NY) at 4°C for 24 hours, biotinylated goat anti-rabbit IgG (Vector, Burlingame, CA) for 1 hour, and acetyl-avidin-biotinylated peroxidase complex (ABC kit, Vector) for another hour. Sections were then processed with a solution containing 0.05% DAB and 0.02% H_2O_2 for visualization of the peroxidase product. Sections were rinsed with 0.1 M PB between each incubation. All incubations except that of the primary antibody were performed at room temperature.

To identify the cholinergic projections to the NMC, tissue sections were processed first with WGA-HRP and then with ChAT immunohistochemistry. After stabilization of the product of WGA-HRP, tissues were rinsed with Tris buffer solution (TBS) three times and then incubated in normal goat serum for 2 hours. Sections were then incubated in

monoclonal ChAT antibody raised from a rat–mouse hybrid (1:1,000; Boehringer Mannheim Bio-chemicals, Indianapolis, IN) at 4°C for 48 hours. After washing with 2% goat normal serum in TBS three times, tissues were incubated in biotinylated anti-rat IgG raised from goat (Vector) for 1 hour and then in the Vectastain ABC kit (Vector) for another hour at room temperature. The final products were visualized by DAB.

As a control, some of the sections were processed as above, with the primary antibody omitted.

A Microplotter 4000+ (Dilog Instruments & Systems, Tallahassee, FL) plotting system connected to a Nikon Optiphot 2 microscope was used to draw the injection and diffusion areas and to plot the distribution of single-labeled WGA-HRP and double-labeled WGA-HRP/glutamate, WGA-HRP/NADPH-d, and WGA-HRP/ChAT neurons. All figures are unretouched photographs and photographic montages.

RESULTS

The WGA-HRP injections in five of the seven cats were centered in the NMC, with variable diffusion to immediately adjacent areas of the inferior olive (IO), raphe magnus, and pyramidal tract (Figs. 1, 2). Of the NMC injections, four (HM11, HM12, HM13, and HM14; Fig. 1) were located at 1.2 mm, and one (HM22; Figs. 1, 2) was located 0.5 mm from the midline. The sixth cat (HM21; Figs. 1, 2) received an injection at the border of nucleus gigantocellularis (NGC) and NMC. The injection site of the seventh cat (HM15) was centered in the pyramidal tract and diffused to the adjacent structures of the IO and the most ventral portion of the NMC (Fig. 1). However, trace amounts of WGA-HRP were found along the needle tract in a dorsocaudal to ventrorostral direction.

The final products after processing with TMB-DAB and histochemical or immunohistochemical staining were black crystals for WGA-HRP, a homogenous blue product for NADPH-d, and a homogenous yellow-brown stain for the glutamate- and ChAT-positive neurons (Figs. 3, 4). Homogeneous brown staining for glutamate and ChAT was not seen in the sections processed without the primary antibody.

Retrogradely labeled neurons in the animals that received a WGA-HRP injection into the NMC were found throughout the brainstem (Figs. 5–7). Heavy projections were present from the mesencephalic reticular formation (MRF), periaqueductal gray (PAG), nuclei pontis centralis oralis (PoO) and caudalis (PoC), and nucleus paragigantocellularis lateralis (NPG). A moderate density of WGA-HRP neurons was found in the retrorubral nucleus (RRN), nucleus parvocellularis (NPC), and in the inferior (VIN), medial (VMN), and lateral (VLN) vestibular nuclei. A light density of WGA-HRP neurons was located in the pedunculopontine (PPN), dorsolateral tegmentum (LDT), and superior vestibular nucleus (VSN). WGA-HRP-labeled cells could be found in the contralateral IO when the WGA-HRP injection included the principal IO (three cats).

In general, the distribution of WGA-HRP neurons in the cat, which had the center of its injection at the border of NGC and NMC (HM21), was similar to that of injections centered in NMC, except that the number of labeled neurons was lower than the number in those that

received injections centered in the NMC in most of the regions that we examined (Table 1). Only a few retrogradely labeled neurons (94 cells) were found in the brainstem in the seventh cat, which was injected in the pyramidal tract (HM15; Table 1).

We previously found that electrical stimulation of the rostral and caudal divisions of NMC are equally potent in producing muscle atonia (Lai et al., 1987). However, glutamate microinjected into the rostral NMC produced a longer lasting and more complete muscle tone suppression than did the injection into the caudal NMC (Lai and Siegel, 1988). Although all sections were plotted, the following description is based on our observations from cat HM11 in which the injection was centered in the rostral NMC. The differences in the distribution of projection neurons in animals with the other injection sites are also described.

Midbrain

WGA-HRP neurons in the Edinger-Westphal nucleus were found exclusively ipsilateral to the injection. WGA-HRP cells were restricted to the most rostral level of the nucleus. A small number of WGA-HRP neurons also contained glutamate (20%). No WGA-HRP neurons were double labeled with NADPH-d.

Retrogradely labeled WGA-HRP neurons in the MRF could be found at a moderate to heavy density in the ipsilateral side and at a moderate density in the contralateral side (Figs. 5–7; A5–A0.5). In general, WGA-HRP-labeled neurons in the MRF were found at a higher density in the cat that received rostral injections than in the cat that received caudal injections (Table 1). Ipsilaterally, the distribution of WGA-HRP neurons differed from rostral to caudal in the midbrain. Rostral to the Edinger-Westphal nucleus, a few WGA-HRP-labeled neurons were found in the MRF. However, between the Edinger-Westphal nucleus and the caudal portion of the substantia nigra, very heavy labeling was found in the dorsal MRF. At caudal levels of the midbrain, WGA-HRP neurons could be seen at a moderate density in the dorsal midbrain, whereas a heavy density was seen in the ventral MRF. Contralaterally, a relatively small number of WGA-HRP neurons was scattered throughout the MRF. Nineteen percent of projection cells in the MRF were double labeled with NADPH-d. Fifty-eight percent of WGA-HRP neurons were double labeled with glutamate (Table 2).

In the RRN, an almost equal number of projection neurons was found on both sides (Figs. 5–7; A3.5–A1.5). Rostrocaudally, more WGA-HRP neurons were found at the level of the pontomesencephalic junction than in the midbrain. Twenty-nine percent and 55% of WGA-HRP neurons were seen in the RRN double stained with NADPH-d and glutamate, respectively (Table 2).

In the PAG, the distribution of WGA-HRP neurons differed as a function of the location of the injection site. In all of the injections, projection neurons in PAG were found at high density at the level of mesopontine junction ipsilaterally and at moderate density at the caudal level. However, the number of retrogradely labeled neurons in the PAG at the superior colliculus level and in the contralateral side depended on the site of the injection. A very high density of WGA-HRP-labeled neuron was found in the cats that received

WGA-HRP injection into the medial NMC (HM21 and HM22; Fig. 7, Table 1), whereas a low density of WGA-HRP neurons was found in the cats that received lateral NMC injections (HM11–HM14; Table 1). A small number of projection cells was double labeled with NADPH-d (4%). Cells double labeled for WGA-HRP and glutamate were concentrated in the ventrolateral part of the PAG. Overall, double-labeled WGA-HRP/glutamate neurons made up 24% of the projections.

Pons

At the pontine level, WGA-HRP cells were found at a very high density in the PoC, PoO, and the Kolliker-Fuse (KF) and medial parabrachial (PBM) area, at a moderate density in the pontine NPC, and at a low density in LDT and PPN. No giant neurons (>50 μ in diameter) in the pons labeled with WGA-HRP.

WGA-HRP neurons in the PoO were found extending from its rostroventral to caudomedial portions. At the level of the mesopontine junction, a very high density of WGA-HRP cells was found in the PoO, bilaterally. Retrogradely labeled WGA-HRP neurons were localized to the ventral portion of the nucleus and dorsal and lateral to the tegmental reticular nucleus. More caudally, very high concentrations of WGA-HRP cells were located contralateral to the injection site (Figs. 5–7; P1.0–P2.0). A moderate density of projection neurons was found on the ipsilateral side. At the most caudal portion of the PoO, WGA-HRP neurons were found to have an opposite laterality distribution compared with the rostral PoO. Intense WGA-HRP labeling at this level was seen in the ipsilateral side, whereas moderate labeling was seen in the contralateral side. Overall, a very high percentage of WGA-HRP cells had glutamate immunoreactivity (51%; Table 2), whereas 30% of WGA-HRP-labeled neurons also contained NADPH-d staining in the PoO.

A very light density of WGA-HRP cells could be found in the ipsilateral LDT. WGA-HRP neurons were found in the rostral LDT, whereas no neuron from the caudal portion of the LDT projected to the NMC (Figs. 5, 6). Double-labeled WGA-HRP/glutamate made up 25% of the projections. Very few double-labeled WGA-HRP/NADPH-d neurons were found in the cat that received rostral-lateral NMC (HM11) injection. Cholinergic neurons in the LDT were not labeled with WGA-HRP in the cats (HM13 and HM14) processed with ChAT immunohistochemistry.

The distribution of WGA-HRP cells in the cuneiformis nucleus (CNF) depended on the injection site. WGA-HRP injected into the lateral portion of the NMC produced a small number (Figs. 5, 6), whereas a relatively large number of WGA-HRP cells was found when the injection was made into the medial portion of the NMC (Fig. 7). More WGA-HRP cells were found ipsilateral than contralateral to the injection site in both medial and lateral NMC injections. However, an almost equal number of WGA-HRP-labeled cells could be found in both sides of the PPN. Double-labeled WGA-HRP and glutamate neurons made up 52% and 15% of projections in the PPN and CNF, respectively. A very small percentage of WGA-HRP neurons had NADPH-d reactivity (11% and 6% in PPN and CNF, respectively). However, 16% of WGA-HRP neurons in the PPN area were double stained with ChAT immunohistochemistry.

In the caudal pons, a very high density of WGA-HRP cells could be found in the PoC, with more projections from the ipsilateral than from the contralateral side. Double-labeled WGA-HRP/NADPH-d neurons made up 8% of the projections. Double-labeled WGA-HRP/glutamate neurons made up 35% (Table 2) of the projection neurons in PoC.

In the locus coeruleus region, a very high concentration of projection cells could be found in the most caudal portion of the KF-PBM nuclei ipsilateral to the injection site in the cats receiving lateral NMC injections (Figs. 5, 6; P2.0–P4.0). A small number of WGA-HRP neurons was found in the cats that received medial NMC injections (Fig. 7). A very high concentration of WGA-HRP neurons was found at the tip of the ventral portion of the brachium conjunctivum and ventral to it, whereas the area medioventral to the brachium conjunctivum had a moderate density of projections (Figs. 5, 6; P3.0). No retrogradely labeled WGA-HRP cell double labeled with NADPH-d. Some WGA-HRP neurons double labeled with glutamate (21%).

Medulla

WGA-HRP neurons in the medullary reticular formation could be seen in the NPC, vestibular complex, NGC, nucleus of solitary tract, principal and spinal trigeminal nuclei, rostral ventrolateral medulla (RVLM), and contralateral NMC.

In the NPC, the numbers of WGA-HRP-labeled neurons were moderate to high at the caudal pontine level and low at the medullary level. The number of WGA-HRP neurons was greater in the ipsilateral than in the contralateral side. Thirteen percent of WGA-HRP neurons double labeled with NADPH-d. Glutamate-immunoreactive neurons made up 54% of the projections.

The vestibular complex had a low to moderate density of WGA-HRP neurons. WGA-HRP neurons could be found at low density in the VSN and at moderate density in the VMN, VLN, and VIN. In the VLN, projections were prominently from the ipsilateral side. Double-labeled WGA-HRP/NADPH-d and WGA-HRP/glutamate neurons made up 5% and 47% of the projection in the VLN, respectively. In the VIN, WGA-HRP neurons could be seen at a moderate density in the cat that received injections into the lateral NMC (Fig. 5; P8.0) but at low density in the cat that received medial NMC injections (Fig. 7; P8.0). A small percentage of the WGA-HRP cells double labeled with NADPH-d (7%). However, a relatively high percentage of the WGA-HRP neurons contained glutamate (43%). The density of WGA-HRP neurons was moderate in the caudal portion and light in the rostral portion of the VMN (Figs. 5, 6; P6.0–P8.0). Most of the WGA-HRP cells in the VMN were found in the area near to the VIN. A small number of WGA-HRP cells were NADPH-d-positive stained. Double-labeled WGA-HRP/glutamate neurons made up 44% of the projection.

The ipsilateral NGC was not included in the data analysis because of its proximity to the injection site. In the contralateral NGC, a moderate to intense density of WGA-HRP neurons was found. No giant neurons in the NGC were retrogradely labeled. Some of the WGA-HRP cells double labeled with NADPH-d (11%). Sixty percent of WGA-HRP neurons also double labeled with glutamate.

Retrogradely labeled WGA-HRP neurons were found in the contralateral side of the NMC. A low to moderate density of WGA-HRP neurons was found in the NMC depending on the injection site. WGA-HRP-labeled neurons were found at low density in the cat that received medial NMC injections (Fig. 7; P7.0–P11.0), whereas a moderate density of retrogradely labeled neurons was found after the lateral NMC injections (Fig. 5). Thirty-five and sixty-eight percent of WGA-HRP neurons were double labeled with NADPH-d and glutamate, respectively.

The RVLM, including the NPG, the adrenergic C1 area, and the ventral surface of the medulla (Ciriello et al., 1986), had a moderate to high number of neurons projecting to the NMC. WGA-HRP labeling in the NPG depended on the site of injection. A moderate to high density of WGA-HRP neurons could be seen in the cats that received a lateral NMC injection (Figs. 5, 6; P8.0–P11.0), whereas a low density of projection cells was seen in the cats that received medial NMC injections (Fig. 7). A very high percentage (57%) of WGA-HRP neurons were also double stained with glutamate. Double-labeled WGA-HRP and NADPH-d-positive neurons were also found, but the number was small. In the C1 area, a low density of WGA-HRP-labeled neuron was found in the contralateral side, whereas a moderate to high density of projection neurons was found in the side ipsilateral to the injection. Forty-four percent of WGA-HRP neurons were double labeled with glutamate in the C1 area. The area near the ventral surface of the medullary reticular formation contains the central chemoreceptor (Loeschcke et al., 1970; Cakar and Terzioglu, 1983; Nattie and Li, 1990; Issa and Remmers, 1992; Sato et al., 1992). A light to moderate density of WGA-HRP neurons could be seen in this area. Some of the WGA-HRP neurons were also double labeled with either glutamate or NADPH-d. Double-labeled WGA-HRP/glutamate and WGA-HRP/NADPH-d made up 53% and 4% of the projection neurons, respectively.

WGA-HRP neurons were found in the contralateral side of IO at the level of the injection. However, this projection could only be seen after the injections that included the principal IO. WGA-HRP cells were small, with an oval shape. A very high percentage (72%) of projection cells double labeled with glutamate.

DISCUSSION

Glutamate has both metabolic and neurotransmitter roles. As discussed previously, the subpopulation of neurons with free glutamate labeled by the present antibody procedure has been hypothesized to use glutamate as a neurotransmitter (Clements et al., 1991; Lai et al., 1993).

Origin of the afferent projections to the NMC

Small differences could be seen in afferents as a function of the portion of the NMC injected. (1) A relatively higher density of WGA-HRP neurons was found in contralateral PAG in the cats that were injected in medial NMC than in those that received lateral NMC injections. (2) In the CNF, a higher number of WGA-HRP neurons was found in the cats that received medial NMC injections. (3) In the KF-PBM area, a very high density of WGA-HRP-labeled neurons was found in the cat that received a lateral NMC injection,

whereas a lower number of retrogradely labeled neurons was found in the cats that received a medial NMC injection.

Although this is the first study of glutamate projections to the NMC, Sakai et al. (1981) demonstrated the afferents to the NMC and Luppi et al. (1988) studied cholinergic, serotonergic, catecholaminergic, enkephalinergic, and CRF projections to NMC by using cholera toxin and immunohistochemistry. Although the anatomical distribution of projection neurons in the present study is similar to the findings by Sakai et al. and Luppi et al., there are some differences. (1) The area of peri-locus coeruleus alpha (PLC) was reported to have intense projections to the NMC in their studies. In contrast, we found that PLC had only light (rostral portion) to moderate (caudal portion) projections to the NMC. (2) The contralateral medial portion of PoO had a very high density of projections to the NMC in the present study, whereas only a light density of projections was reported by Luppi et al. (1988). (3) We found that the RVLM also contained a very high density of WGA-HRP neurons bilaterally. In contrast, they did not find any neurons from RVLM projecting to the NMC. Studies on the rat using the anterograde transport lectin *Phaseolus vulgaris*–leucoagglutine (PHA-L) technique have reported projections from RVLM to the nucleus gigantocellularis alpha (Zagy, 1992), which corresponds to the NMC in cat.(4) In contrast to the study by Luppi et al. (1988), we found that the projection neurons from the LDT to the NMC was noncholinergic.

The projections to the nucleus gigantocellularis alpha and ventralis in the rat have been studied by retrograde transport WGA-HRP or anterograde tracer injection techniques. Anterograde PHA-L and autoradiographic studies have demonstrated that the nucleus gigantocellularis alpha and ventralis in the rat receive moderate to strong innervation from the CNF (Bernard et al., 1989), PoO (Jones and Yang, 1985), PPN (Rye et al., 1988), KF (Grofova and Keane, 1991; Korte et al., 1992), dorsal raphe (Vertes and Kocsis, 1994), PAG (Van Bockstaele et al., 1991), and C1 cell group (McKellar and Loewy, 1982). Retrograde transport HRP studies have shown that neurons in the PAG (Zeng et al., 1991) and PoO (Gallager and Pert, 1978; Bayev et al., 1988) project to the nucleus gigantocellularis alpha and ventralis in the rat. Projection from the MRF to the medial ventral medulla has also been found in the monkey (Chung et al., 1983).

Neurons double labeled with NADPH-d and WGA-HRP could be seen throughout the brainstem, although their number was small. NADPH-d-positive neurons contain NO synthase (Hope et al., 1991). Immunohistochemical studies have shown that NADPH-d-positive neurons coexist with substance P and enkephalin in the laterodorsal PAG (Moss and Basbaum, 1983), acetylcholine in the PPN and LDT (Vincent et al., 1983; Reiner and Vincent, 1987; Mesulam et al., 1989), neuropeptide Y and somatostatin in forebrain (Scott et al., 1987) and striatum (Kowall et al., 1987). However, double-labeled WGA-HRP/NADPH-d neurons in the LDT in the present study do not appear to represent a cholinergic projection because no WGA-HRP/ChAT-labeled neurons were found in the tissue processed with ChAT. However, a significant percentage of the double-labeled WGA-HRP/NADPH-d neurons in the PPT may be cholinergic.

Abundant glutamatergic projections to the NMC were found throughout the brainstem. However, the PoO had the highest density and percentage of WGA-HRP/glutamate projections to NMC.

WGA-HRP neurons in the IO may not project to the NMC. Anatomical studies have demonstrated that neurons in the principal nucleus of the IO send fibers across the midline and project to the cerebellum (Noback and Demarest, 1981). The crossing fibers of the principal IO may be damaged by injection needle penetration and retrogradely transport HRP to the contralateral IO. No projection cells were found in the cats (four cases) in which the injection did not include the principal nucleus of the IO.

Physiological implications

Our previous study has demonstrated that microinjection of cholinergic agonists into the NMC produces increases in heart rate and decreases in blood pressure. This cholinergic-induced cardiovascular response has been found to be dose dependent and blocked by previous administration of the cholinergic antagonist atropine (Lai and Siegel, 1990). The cholinergic projections from the PPN to the NMC found in the present study may participate in the regulation of cardiovascular system.

The nucleus magnocellularis of the medulla has been implicated as the final common pathway responsible for muscle atonia during REM sleep. Electrophysiological studies have shown that the NMC receives a monosynaptic projection from the pontine reticular formation (Sakai et al., 1981) and in turn projects to the spinal cord (Tohyama et al., 1979). This pathway produces hyperpolarization of spinal motoneurons in REM sleep (Chase et al., 1981). In the decerebrate cat, we found that electrical stimulation of the RRN, PoC, PoO, PPN, and ventral part of paralemniscal tegmental field produces muscle tone suppression at low threshold and short latency (Lai and Siegel, 1990). In accord with our physiological findings, the present study demonstrated that the NMC receives a moderate to intense projection from all these mesopontine muscle tone suppression areas. This projection includes glutamatergic and NADPH-d cells.

Previous microinjection studies have shown that glutamate injection into the NMC produces muscle atonia and that this effect is mediated by non-NMDA receptors (Lai and Siegel, 1988). Activation of NMDA receptors in the NMC produces increased muscle tone and locomotion (Lai and Siegel, 1991). In the present study, we found that a very high percentage of the neurons projecting from RRN, PPN, and PoO to NMC was glutamatergic. We hypothesize that glutamate release from the terminals of neurons in these rostral areas into NMC is responsible for the muscle atonia and phasic motor events of REM sleep.

The PoO acetylcholine effect on muscle atonia may be mediated through a glutamatergic projection to the NMC because we have found that microinjection of glutamate antagonists into the NMC blocks pontine carbachol-induced muscle atonia (Lai and Siegel, 1988). The dense and high percentage of glutamatergic projections from the PoO to the NMC in the present study supports our hypothesis that activation of pontine glutamatergic neurons by acetylcholine participates in muscle atonia mediated through the NMC.

We found major projections from the RVLM to the NMC. The RVLM has been identified as a sympathoexcitatory area (Ross et al., 1984; Routledge and Marsden, 1987) with input from baroreceptors and chemoreceptors (Ciriello et al., 1986; Sun and Guyenet, 1987). In a previous study (Lai et al., 1987), it was found that increases in blood pressure produce reductions in muscle tone. We also found that decreased blood pressure reverses the muscle tone suppression produced by NMC stimulation, thereby producing facilitation instead. This relationship between sympathetic activity and muscle tone has also been reported in normal human subjects (Somers et al., 1993). On the basis of our previous and present studies, we hypothesized that neuronal activity in the RVLM not only excites preganglionic neurons in the intermediolateral column, thereby increasing blood pressure, but also activates NMC neurons, which hyperpolarize spinal motoneurons and produce suppression of muscle tone. We had hypothesized that the reversal of muscle response to NMC stimulation was mediated through the central chemoreceptor (Lai et al., 1987). Our present finding that neurons in the central chemoreceptor area project to the NMC is consistent with this hypothesis.

Obstructive sleep apnea, which is accompanied by a loss of tone in a number of upper airway muscles, typically occurs during REM sleep or at non-REM-to-REM transitions (Issa and Sullivan, 1984). The increase in upper airway resistance, which causes airway collapse, results from the depression of hypoglossal motor neuron and pharyngeal muscle activity (Kuna and Sant'Ambrogio, 1991). Hypoglossal motoneurons have been reported to receive NMC projections (Manaker and Tischler, 1993). These NMC projections may underlay the neurological aspects of sleep apnea.

Neuronal firing in NMC coincident with REM sleep and cataplectic attacks in the narcoleptic dog have been reported (Siegel et al., 1991), which is consistent with the hypothesis that these neurons mediate the muscle tone suppression of cataplexy and REM sleep. Myoclonic jerks or regular coordinated muscle activity elicited by damage of the ventral mesopontine junction in the decerebrate cat (Lai and Siegel, 1997a) can be blocked by microinjection of DL-2-amino-5-phosphanovaleric acid, a specific NMDA antagonist, and nonNMDA agonists into NMC (Lai and Siegel, 1997b). Therefore, the glutamatergic system passing through NMC that has been identified in the current studies may mediate the normal muscle tone suppression of REM sleep and such pathologies of state-related muscle control as cataplexy, REM behavior disorder, and sleep apnea.

ACKNOWLEDGMENTS

This study was supported by grant NSC83-0412-B-075A-033, Taiwan (Y.Y.L.) and grants USPHS HL41370, HL60296, NS14610, and the Medical Research Service of the Veterans Administration (J.M.S.).

Grant number:

NSC83-0412-B-075A-033; Grant sponsor: Medical Research Service of the Veterans Administration; Grant numbers: USPHS HL41370 and NS14610.

Abbreviations

3	oculomotor nucleus
3N	third nerve

4	trochlear nucleus
5M	motor trigeminal nucleus
5P	principal sensory trigeminal nucleus
5SP	spinal trigeminal nucleus
5ST	spinal trigeminal tract
7	facial nucleus
7N	facial nerve
AQ	aqueduct
BC	brachium conjunctivum
CD	nucleus medullae oblongatae centralis, dorsalis
CNF	nucleus cuneiformis
CV	nucleus medullae oblongatae centralis, ventralis
CX	cuneate nucleus
DRN	dorsal raphe nucleus
EW	nucleus Edinger-Westphal
IC	inferior colliculus
ICA	interstitial nucleus of Cajal
IO	inferior olivary nucleus
IP	interpeduncle nucleus
KF	Kolliker-Fuse nucleus
LC	locus coeruleus
LDT	laterodorsal tegmentum
LLV	ventral nucleus of lateral lemniscus
LR	rostral linear nucleus
MRF	mesencephalic reticular formation
NGC	nucleus gigantocellularis
NMC	nucleus magnocellularis
NPC	nucleus parvocellularis
NPG	nucleus paragigantocellularis lateralis

NTS	nucleus of solitary tract
P	pyramidal tract
PAG	periaqueductal gray
PBM	medial parabrachial nucleus
PCN	nucleus of the posterior commissure
PG	pontine gray
PLC	peri-locus coeruleus alpha
PoC	nucleus pontis centralis caudalis
PoO	nucleus pontis centralis oralis
PPN	pedunculopontine nucleus
PT	medial pretectal area
RB	restiform body
RN	red nucleus
RRN	retrorubral nucleus
RVLM	rostral ventrolateral medulla
SC	superior colliculus
SNC	substantia nigra, compacta
SNL	substantia nigra, lateralis
SNR	substantia nigra, reticulata
SO	superior olive
TB	trapezoid body
TRC	tegmental reticular nucleus, central division
VIN	inferior vestibular nucleus
VLN	lateral vestibular nucleus
VMN	medial vestibular nucleus
VSN	superior vestibular nucleus
WGA–HRP	wheat germ agglutinin–horseradish peroxidase

LITERATURE CITED

Atsuta Y, Garcia-Rill E, Skinner RD. 1990. Characteristics of electrically induced locomotion in rat in vitro brain stem–spinal cord preparation. J Neurophysiol 64:727–735. [PubMed: 2230919]

Bayev KV, Beresovskii VK, Kebkalo TG, Savoskina LA. 1988. Afferent and efferent connections of brainstem locomotor regions: Study by means of horseradish peroxidase transport technique. Neuroscience 26:871–891. [PubMed: 3200433]

Berman AL. 1968. The brain stem of the cat. Madison: University of Wisconsin Press.

Bernard JF, Peschanski M, Besson JM. 1989. Afferents and efferents of the rat cuneiformis nucleus: an anatomical study with reference to pain transmission. Brain Res 490:181–185. [PubMed: 2474360]

Cakar L, Terzioglu M. 1983. Localization of CO_2 sensitive units in the rostral medullary chemosensitive area of the cat. In: Schlaefke ME, Koepchen HP, See WR, editors. Central neuron environment and the control systems of breathing and circulation. Berlin: Springer-Verlag. p 52–60.

Chase MH, Enomoto S, Murakami T, Nakamura Y, Taira M. 1981. Intracellular potential of medullary reticular neurons during sleep and wakefulness. Exp Neurol 71:226–233. [PubMed: 7449896]

Chung JM, Kevetter GA, Yezierski RP, Haber L-RH, Martin RF, Willis WD. 1983. Midbrain nuclei projecting to the medial medulla oblongata in the monkey. J Comp Neurol 214:93–102. [PubMed: 6841679]

Ciriello J, Caverson MM, Polosa C. 1986. Function of the ventrolateral medulla in the control of the circulation. Brain Res Rev 11:359–391.

Clements JR, Toth DD, Highfield DA, Grant SJ. 1991. Glutamate-like immunoreactivity is present within cholinergic neurons of the laterodorsal tegmental and pedunculopontine nuclei. In: Kalivas P, Hanin I, Napier T, editors. The basal forebrain: anatomy to function. New York: Plenum Press. p 127–142.

Datta S, Patterson EH, Siwek DF. 1997. Endogenous and exogenous nitric oxide in the pedunculopontine tegmentum induces sleep. Synapse 27:69–78. [PubMed: 9268066]

Dawson TM, Bredt DS, Fotuhi M, Hwang PM, Snyder SH. 1991. Nitric oxide synthase and neuronal NADPH diaphorase are identical in brain and peripheral tissues. Proc Natl Acad Sci USA 88:7797–7801. [PubMed: 1715581]

Dzoljic E, van Leeuwen R, de Vries R, Dzoljic MR. 1997. Vigilance and EEG power in rats: effects of potent inhibitors of the neuronal nitric oxide synthase. Naunyn-Schmiedebergs Arch Pharmacol 356:56–61. [PubMed: 9228190]

Dzoljic MR, de Vries R, van Leeuwen R. 1996. Sleep and nitric oxide: effects of 7-nitro indazole, inhibitor of brain nitric acid synthase. Brain Res 718:145–150. [PubMed: 8773777]

Dzulfic MR, de Vries R, van Leeuwen R. 1996. Sleep and nitric oxide: effects of 7-nitro indazole, inhibitor of brain nitric oxide synthase. Brain Res 718:145–150. [PubMed: 8773777]

Gallager DW, Pert A. 1978. Afferents to brain stem nuclei (brain stem raphe, nucleus reticularis pontis caudalis and nucleus gigantocellularis) in the rat as demonstrated by microiontophoretically applied horseradish peroxidase. Brain Res 144:257–275. [PubMed: 646855]

Grofova I, Keane S. 1991. Descending brainstem projections of the pedunculopontine tegmental nucleus in the rat. Anat Embryol 184:275–290.

Hajnik T, Lai YY, Siegel JM. 1995. Atonia-related regions in the rodent pons and medulla. Sleep Res 24A:26.

Hope BT, Michael GJ, Knigge KM, Vincent SR. 1991. Neuronal NADPH-diaphorase is a nitric oxide synthase. Proc Natl Acad Sci USA 88:2811–2814. [PubMed: 1707173]

Issa FG, Remmers JE. 1992. Identification of a subsurface area in the ventral medulla sensitive to local changes in Pco_2. J Appl Physiol 72:439–446. [PubMed: 1559917]

Issa FG, Sullivan CE. 1984. Upper airway closing pressures in obstructive sleep apnea. J Appl Physiol 57:520–527. [PubMed: 6381440]

Jones BE, Yang T-Z. 1985. The efferent projections from the reticular formation and the locus coeruleus studied by anterograde and retrograde axonal transport in the rat. J Comp Neurol 242:56–92. [PubMed: 2416786]

Kapas L, Krueger JM. 1996. Nitric oxide donors SIN-1 and SNAP promote nonrapid-eye-movement sleep in rats. Brain Res Bull 41:293–298. [PubMed: 8924040]

Kapas L, Fang J, Krueger JM. 1994a. Inhibition of nitric oxide synthesis inhibits rat sleep. Brain Res 664:189–196. [PubMed: 7534601]

Kapas L, Shibata M, Kimura M, Krueger JM. 1994b. Inhibition of nitric oxide synthesis suppresses sleep in rabbits. Am J Physiol 266:R151–R157. [PubMed: 8304536]

Kinjo N, Atsuta Y, Webber M, Kyle R, Skinner RD, Garcia-Rill E. 1990. Medioventral medulla-induced locomotion. Brain Res Bull 24:509–516. [PubMed: 2186847]

Korte SM, Jaarsma D, Luiten PGM, Bohus B. 1992. Mesencephalic cuneiform nucleus and its ascending and descending projections serve stress-related cardiovascular responses in the rat. J Auton Nerv Syst 41:157–176. [PubMed: 1491112]

Kowall NW, Ferrante RJ, Beal MF, Richardson EP Jr, Sofroniew MV, Cuello AC, Martin JB. 1987. Neuropeptide Y, somatostatin, and reduced nicotinamide adenine dinucleotide phosphate diaphorase in the human striatum: a combined immunocytochemical and enzyme histochemical study. Neuroscience 20:1017–1025.

Kuna ST, Sant'Ambrogio G. 1991. Pathophysiology of upper airway closure during sleep. JAMA 266:1384–1389. [PubMed: 1880868]

Lai YY, Siegel JM. 1988. Medullary regions mediated muscle atonia. JNeurosci 8:4790–4796. [PubMed: 2904495]

Lai YY, Siegel JM. 1990. Cardiovascular and muscle tone changes produced by microinjection of cholinergic and glutamatergic agonists in dorsolateral pons and medial medulla. Brain Res 514:27–36. [PubMed: 1972638]

Lai YY, Siegel JM. 1991. Pontomedullary glutamate receptors mediating locomotion and muscle tone suppression. J Neurosci 11:2931–2937. [PubMed: 1679125]

Lai YY, Siegel JM. 1992. Corticotropin-releasing factor mediated muscle atonia in pons and medulla. Brain Res 575:63–68. [PubMed: 1504782]

Lai YY, Siegel JM. 1997a. Brainstem-mediated locomotion and myoclonic jerks. I. Neural substrates. Brain Res 745:257–264. [PubMed: 9037417]

Lai YY, Siegel JM. 1997b. Brainstem-mediated locomotion and myoclonic jerks. II. Pharmacological effects. Brain Res 745:265–270. [PubMed: 9037418]

Lai YY, Siegel JM, Wilson WJ. 1987. Effect of blood pressure on medial medulla-induced muscle atonia. J Am Physiol 252:H1249–H1257.

Lai YY, Clements JR, Siegel JM. 1993. Glutamatergic and cholinergic projections to the pontine inhibitory area identified with horseradish peroxidase retrograde transport and immunohistochemistry. J Comp Neurol 336:321–330. [PubMed: 7505295]

Leonard TO, Lydic R. 1997. Pontine nitric oxide modulates acetylcholine release, rapid eye movement sleep generation, and respiratory rate. J Neurosci 17:774–785. [PubMed: 8987799]

Loeschcke HH, De Lattre J, Schlaefke ME, Trough CO. 1970. Effects on respiration and circulation of electrically stimulating the ventral surface of the medulla oblongata. Respir Physiol 10:184–197. [PubMed: 5505806]

Luppi P-H, Sakai K, Fort P, Salvert D, Jouvet M. 1988. The nuclei of origin of monoaminergic, peptidergic, and cholinergic afferents to the cat nucleus reticularis magnocellularis: a double-labeling study with cholera toxin as a retrograde tracer. J Comp Neurol 277:1–20. [PubMed: 3198792]

Manaker S, Tischler LJ. 1993. Origin of serotoninergic afferents to the hypoglossal nucleus in the rat. J Comp Neurol 334:466–476. [PubMed: 8376628]

McKellar S, Loewy AD. 1982. Efferent projections of the A1 catecholamine cell group in the rat: an autoradiographic study. Brain Res 241:11–29. [PubMed: 6809224]

Mesulam M-M. 1978. Tetramethylbenzidine for horseradish peroxidase neurohistochemistry: a non-carcinogenic blue reaction-product with superior sensitivity for visualizing neural afferents and efferents. J Histochem Cytochem 26:106–117. [PubMed: 24068]

Mesulam M-M, Geula C, Bothwell MA, Hersh L. 1989. Human reticular formation: cholinergic neurons of the pedunculopontine and laterodorsal tegmental nuclei and some cytochemical comparisons to forebrain cholinergic neurons. J Comp Neurol 281:611–633.

Moruzzi B, Magoun HW. 1949. Brain stem reticular formation and activation of the EEG. EEG Clin Neurophysiol 1:455–473.

Moss MS, Basbaum AI. 1983. The peptidergic organization of the cat periaqueductal gray: II. The distribution of immunoreactive substance P and vasoactive intestinal polypeptide. J Neurosci 7:1437–1449.

Nattie EE, Li A. 1990. Ventral medulla sites of muscarinic receptor subtypes involved in cardiorespiratory control. J Appl Physiol 69:33–41. [PubMed: 2118496]

Newman DB. 1985. Distinguishing rat brainstem reticulospinal nuclei by their neuronal morphology. I. Medullary nuclei. J Hirnforsch 26:187–226. [PubMed: 2410489]

Noback CR, Demarest RJ. 1981. The human nervous system: basic principles of neurobiology, 3rd ed. New York: McGraw-Hill. p 268–321.

Noga BR, Kettler J, Jordan LM. 1988. Locomotion produced in mesencephalic cats by injections of putative transmitter substances and antagonists into the medial reticular formation and the pontomedullary locomotor strip. J Neurosci 8:2074–2086. [PubMed: 2898514]

Perreault M-C, Drew T, Rossignol S. 1993. Activity of medullary reticulospinal neurons during fictive locomotion. J Neurophysiol 69:2232–2247. [PubMed: 8350141]

Reiner PB, Vincent SR. 1987. Topographic relations of cholinergic and noradrenergic neurons in the feline pontomesencephalic tegmentum: an immunohistochemical study. Brain Res Bull 19:705–714. [PubMed: 2894238]

Ross CA, Ruggiero DA, Park DH, Joh TH, Sved AF, Fernandez-Pardal J, Saavedra JM, Reis DJ. 1984. Tonic vasomotor control by the rostral ventrolateral medulla: effect of electrical and chemical stimulation of the area containing C1 adrenaline neurons on arterial pressure, heart rate, and plasma catecholamines and vasopressin. J Neurosci 4:474–494. [PubMed: 6699683]

Routledge C, Marsden CA. 1987. Electrical stimulation of the rostral ventrolateral medulla of the rat increases mean arterial pressure and adrenaline release in the posterior hypothalamus. Neuroscience 20:457–466. [PubMed: 2438591]

Rye DB, Clifford BS, Wainer BH. 1984. Stabilization of the tetramethylbenzidine (TMB) reaction product: application for retrograde and anterograde tracing, and combination with immunohistochemistry. J Histochem Cytochem 32:1145–1153. [PubMed: 6548485]

Rye DB, Lee HJ, Saper CB, Wainer BH. 1988. Medullary and spinal efferents of the pedunculopontine tegmental nucleus and adjacent mesopontine tegmentum in the rat. J Comp Neurol 269:315–341. [PubMed: 2453532]

Sakai K, Sastre JP, Kanamori N, Jouvet M. 1981. State-specific neurons in the ponto-medullary reticular formation with special reference to the postural atonia during paradoxical sleep in the cat. In: Pompeiano O, Ajmone-Marsan C, editors. Brain mechanisms and perceptual awareness. New York: Raven Press. p 405–429.

Sato M, Severinghaus JW, Basbaum AI. 1992. Medullary CO_2 chemoreceptor neuron identification by c-fos immunocytochemistry. J Appl Physiol 73:96–100. [PubMed: 1506406]

Scherer-Singler U, Vincent SR, Kimura H, McGeer EG. 1983. Demonstration of a unique population of neurons with NADPH-diaphorase histochemistry. J Neurosci Methods 9:229–234. [PubMed: 6363828]

Scott JW, McDonald JK, Pemberton RL. 1987. Short axon cells of the rat olfactory bulb display NADPH-diaphorase activity, neuropeptide Y-like immunoreactivity, and somatostatin-like immunoreactivity. J Comp Neurol 260:378–391. [PubMed: 3298331]

Siegel JM, Wheeler RL, McGinty DJ. 1979. Activity of medullary reticular formation neurons in the unrestrained cat during waking and sleep. Brain Res 179:49–60. [PubMed: 228803]

Siegel JM, Nienhuis R, Fahringer HM, Paul R, Shiromani P, Dement WC, Mignot E, Chiu C. 1991. Neuronal activity in narcolepsy: identification of cataplexy-related cells in the medial medulla. Science 252:1315–1318. [PubMed: 1925546]

Somers VK, Dyken ME, Mark AL, Abboud FM. 1993. Sympathetic-nerve activity during sleep in normal subjects. N Engl J Med 328:303–307. [PubMed: 8419815]

Sun M-K, Guyenet PG. 1987. Arterial baroreceptor and vagal inputs to sympathoexcitatory neurons in rat medulla. Am J Physiol 252:R699–R709. [PubMed: 3032005]

Taber E 1961. The cytoarchitecture of the brain stem of the cat. I. Brain stem nuclei of cat. J Comp Neurol 116:27–70. [PubMed: 13774738]

Tohyama M, Sakai K, Salvert D, Touret M, Jouvet M. 1979. Spinal projections from the lower brainstem in the cat as demonstrated by the horseradish peroxidase technique I. Origins of the reticulospinal tracts and their funicular trajectories. Brain Res 173:383–403. [PubMed: 487101]

Van Bockstaele EJ, Aston-Jones G, Pieribone VA, Ennis M, Shipley MT. 1991. Subregions of the periaqueductal gray topographically innervate the rostral ventral medulla in the rat. J Comp Neurol 309:305–327. [PubMed: 1717516]

Vertes RP, Kocsis B. 1994. Projections of the dorsal raphe nucleus to the brainstem: PHA-L analysis in the rat. J Comp Neurol 340:11–26. [PubMed: 8176000]

Vincent SR, Satoh K, Armstrong DM, Fibiger HC. 1983. NADPH-diaphorase: a selective histochemical marker for the cholinergic neurons of the pontine reticular formation. Neurosci Lett 43:31–36. [PubMed: 6366624]

Zagy A 1992. Interconnections between rostral ventral medullary nuclei in the rat: An anterograde tract tracing study. Soc Neurosci Abstr 18:683.

Zeng S-L, Li YQ, Rao Z-R, Shi J-W. 1991. Projections from serotonin- and substance P-like immunoreactive neurons in the midbrain periaqueductal gray onto the nucleus reticularis gigantocellularis pars alpha in the rat. Neurosci Lett 131:205–209. [PubMed: 1722297]

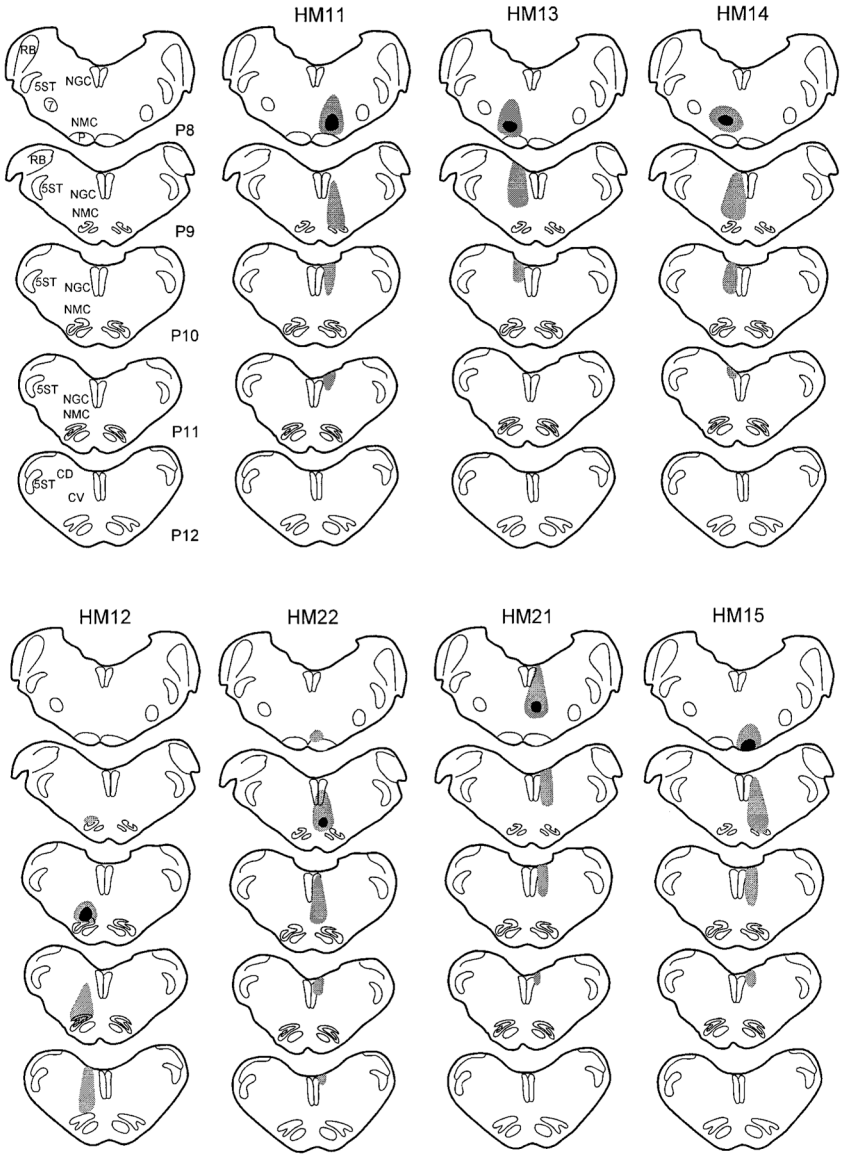

Fig. 1.

Coronal sections show the wheat germ agglutinin–horseradish peroxidase injection sites in seven cats. The black areas represent the injection centers, and gray areas represent the areas of diffusion and needle tract. P, millimeters posterior to stereotaxic 0. For abbreviations, see list.

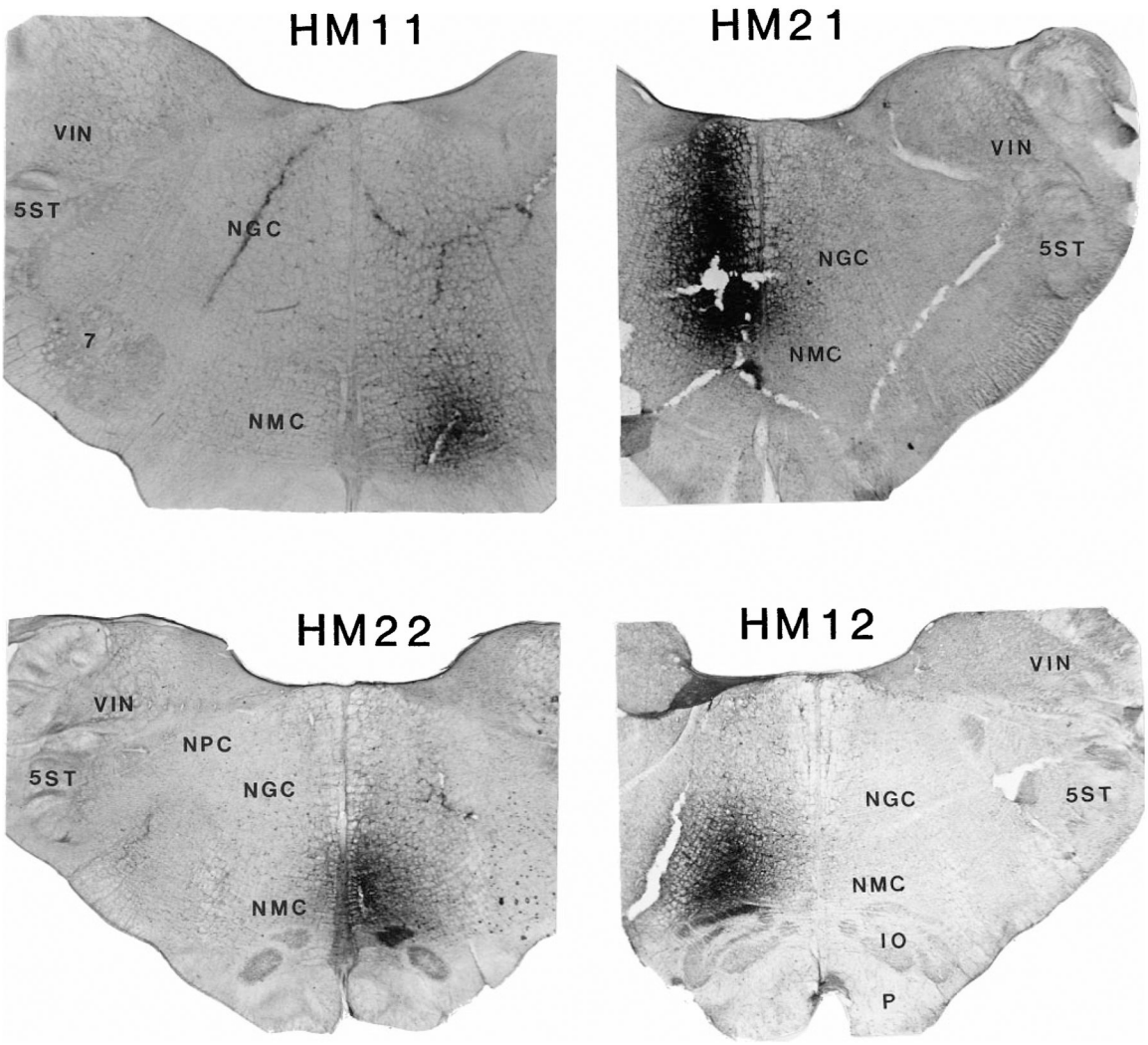

Fig. 2.

Four representative wheat germ agglutinin–horseradish peroxidase injection sites. Injection sites are located in the lateral rostral nucleus magnocellularis (NMC; HM11), lateral caudal NMC (HM12), and medial NMC (HM22) and at the border of the nucleus gigantocellularis (NGC) and NMC (HM21). For abbreviations, see list.

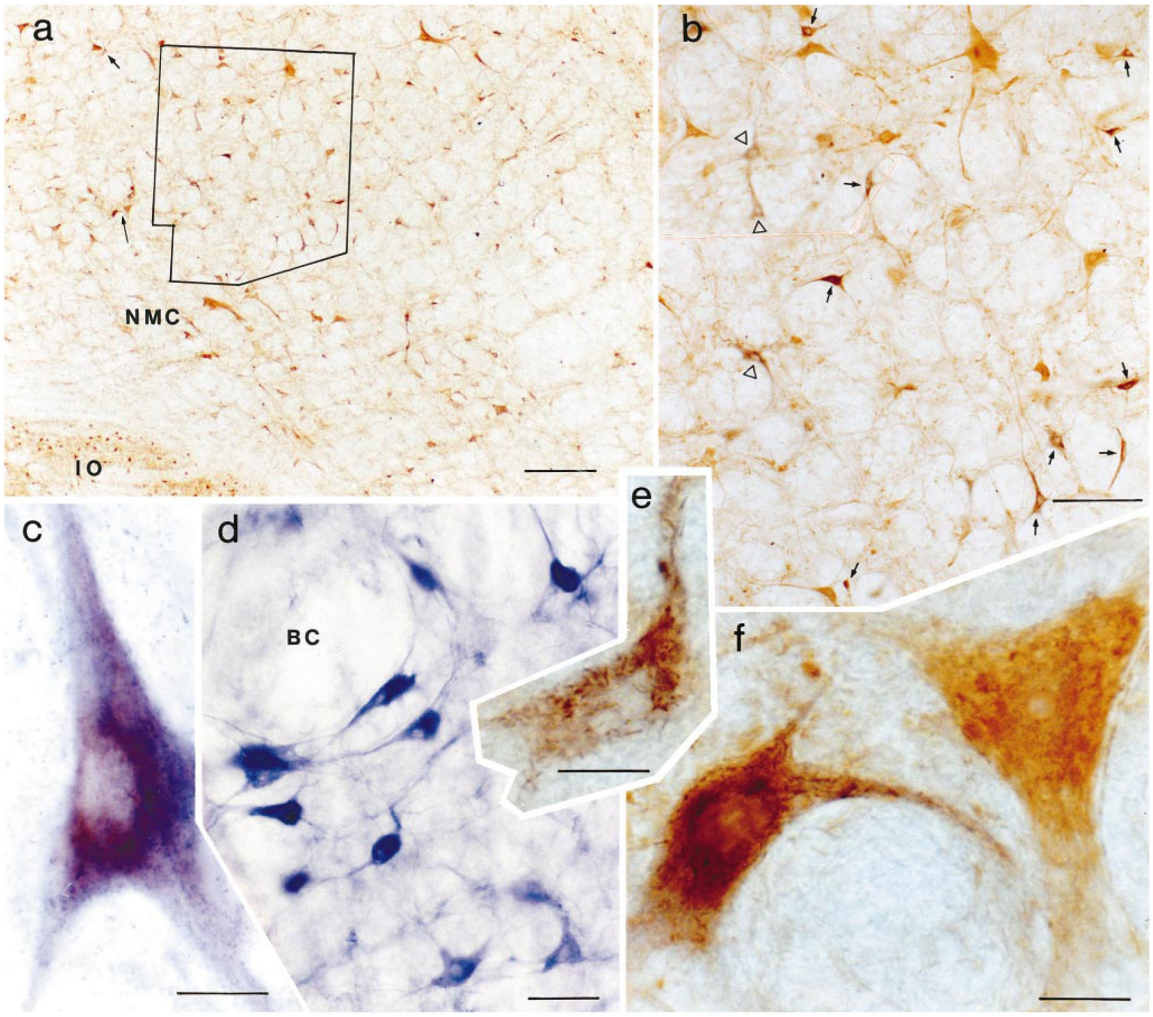

Fig. 3.

Photomicrographs showing wheat germ agglutinin–horseradish peroxidase (WGA-HRP) cells and cells double labeled with either glutamate or nicotinamide adenine dinucleotide phosphate-diaphorase (NADPH-d). **a:** Low magnification photomicrograph taken from the nucleus magnocellularis contralateral to the injection site. The section level is also shown in Figure 5, part 2 as level P10.0. **b:** Higher magnification photomicrograph taken of the area outlined within a. Many neurons labeled with WGA-HRP (open triangles) or WGA-HRP and glutamate (arrows) could be seen in this area. **c:** Double-labeled NADPH-d and WGA-HRP neurons in the nucleus paragigantocellularis contralateral to the injection site. Crystalline tetramethyl benzidine products are superimposed on the light-blue NADPH-d reaction. **d:** NADPH-d-positive neurons in the pedunculopontine nucleus. NADPH-d-positive neurons in the nucleus are large and deep blue and have several processes. **e:** High magnification photomicrograph shows WGA-HRP-labeled neuron shown in a (short arrow). **f:** High magnification photomicrograph showing homogenous yellow glutamate-immunoreactive neuron and double-labeled glutamate/WGA-HRP neuron shown in a (long arrow). For abbreviations, see list. Scale bars = 200 μ in a, 100 μ in b, 20 μ in c–f.

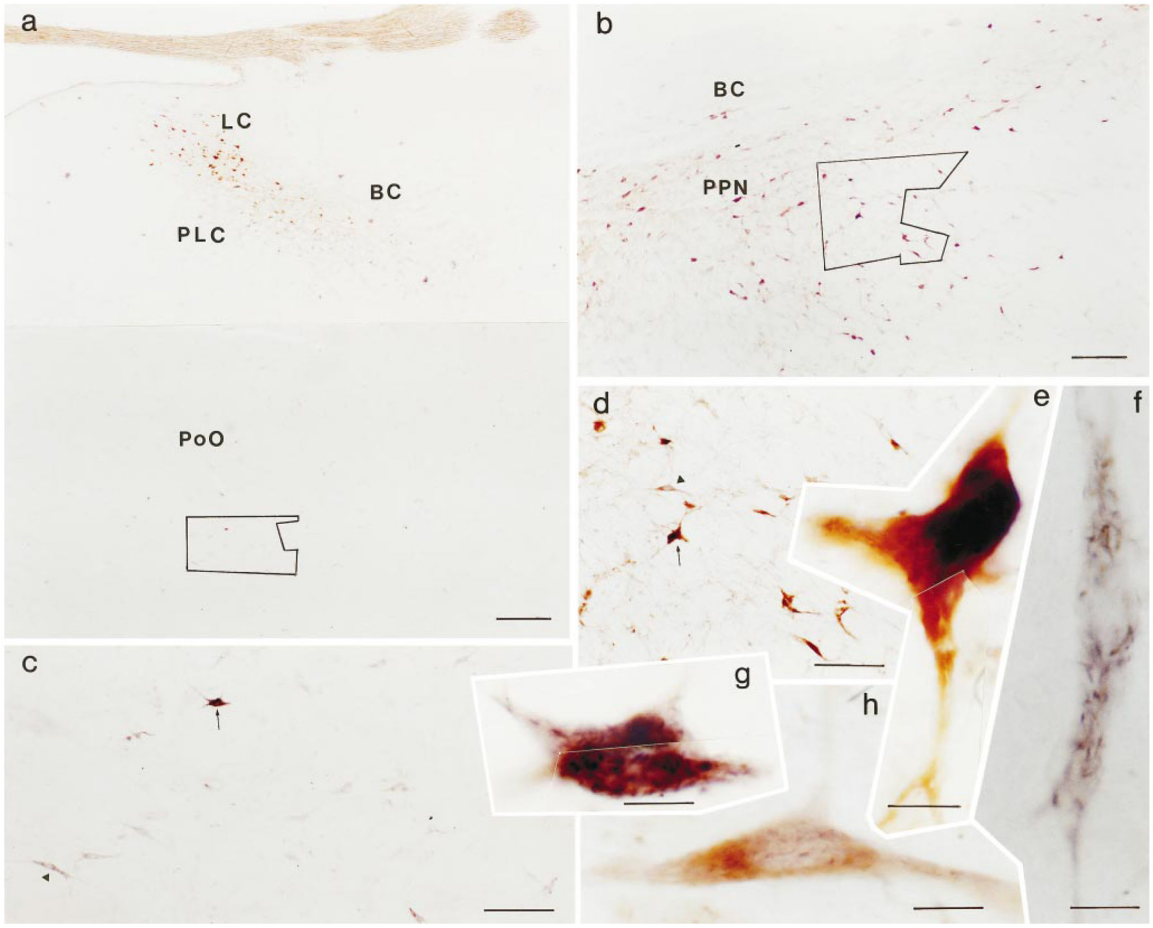

Fig. 4.

Photomicrographs showing wheat germ agglutinin–horseradish peroxidase (WGA-HRP) cells and cells labeled with choline acetyltransferase (ChAT). **a:** Low magnification photomicrographs show the pontine area at the level of the locus coeruleus. ChAT-positive neurons were located in the dorsolateral pons, whereas WGA-HRP labeled neurons were located in the medial pons. These cell types cannot be distinguished at low magnification. **b:** Low magnification photomicrograph taken from the pedunculopontine nucleus. **c:** Higher magnification photomicrograph taken from the area outlined in a. Many neurons labeled with WGA-HRP can be seen in this area. **d:** Higher magnification photomicrograph taken from the area outlined in b. **e:** Neuron labeled with ChAT taken shown in d (arrow, rotated in e) has a homogeneous yellow-brown reaction. **f,g:** Crystalline WGA-HRP products can be seen in the neurons shown in c (triangle in f, arrow in g). **h:** High magnification photomicrograph shows neuron labeled with WGA-HRP and ChAT. WGA-HRP products are superimposed on the homogeneous yellow ChAT reaction. For abbreviations, see list. Scale bars = 400 μ in a, 200 μ in b, 100 μ in c,d, 20 μ in e–h.

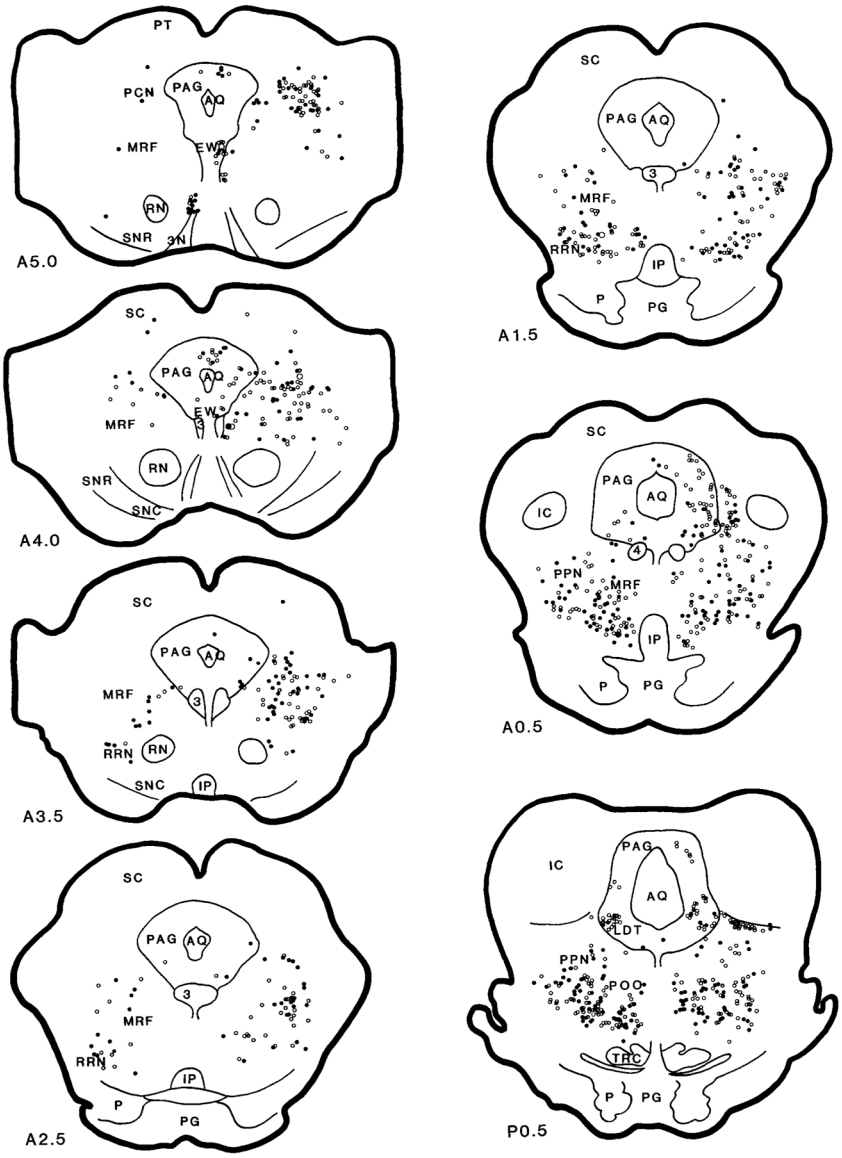

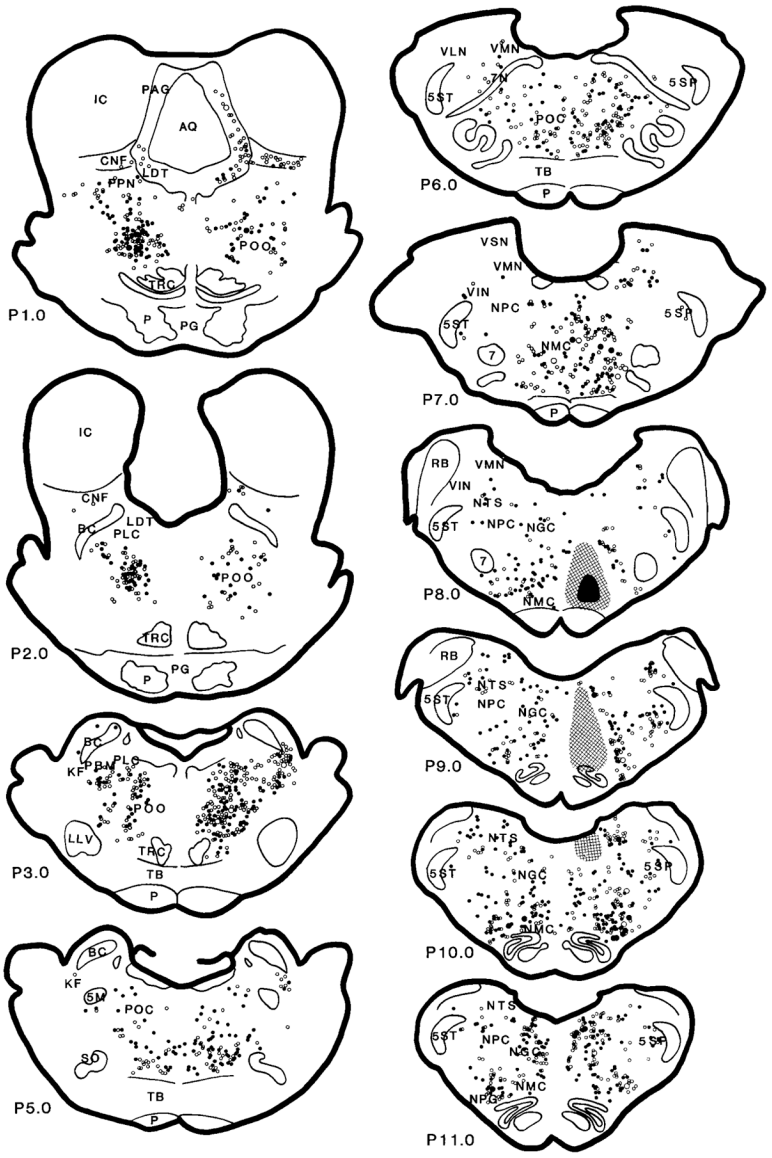

Fig. 5.

Serial coronal sections showing the distribution of the projection neurons from the brainstem to the nucleus magnocellularis (case HM11). The sections were reconstructed according to Berman's atlas (1968). Anatomical nomenclature was based on that of Taber (1961) and Berman (1968). Open circles represent wheat germ agglutinin–horseradish peroxidase (WGA-HRP) and filled circles represent WGA-HRP neurons double labeled with glutamate. The small and large symbols represent one and five neurons, respectively. The black and gray areas represent the injection center and diffused areas, respectively. The sections were taken from cat HM11. A and P, millimeters anterior and posterior, respectively, to stereotaxic 0. For abbreviations, see list.

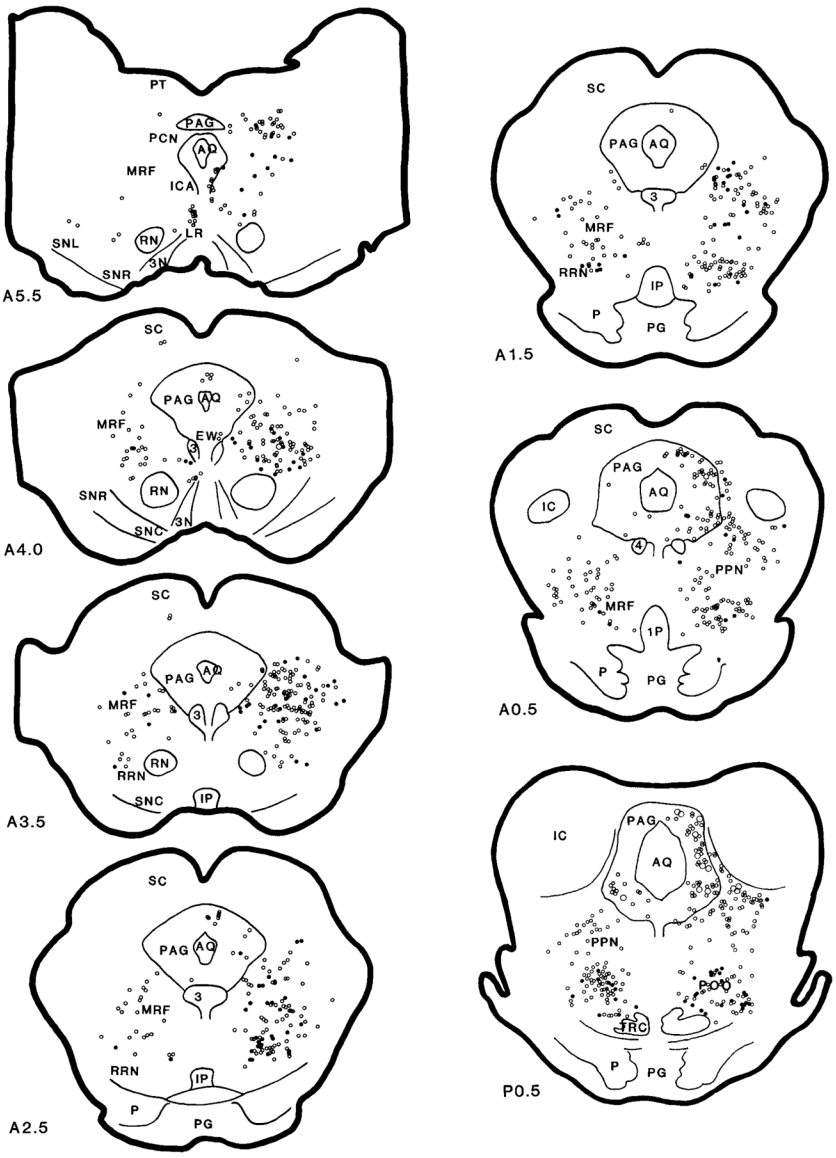

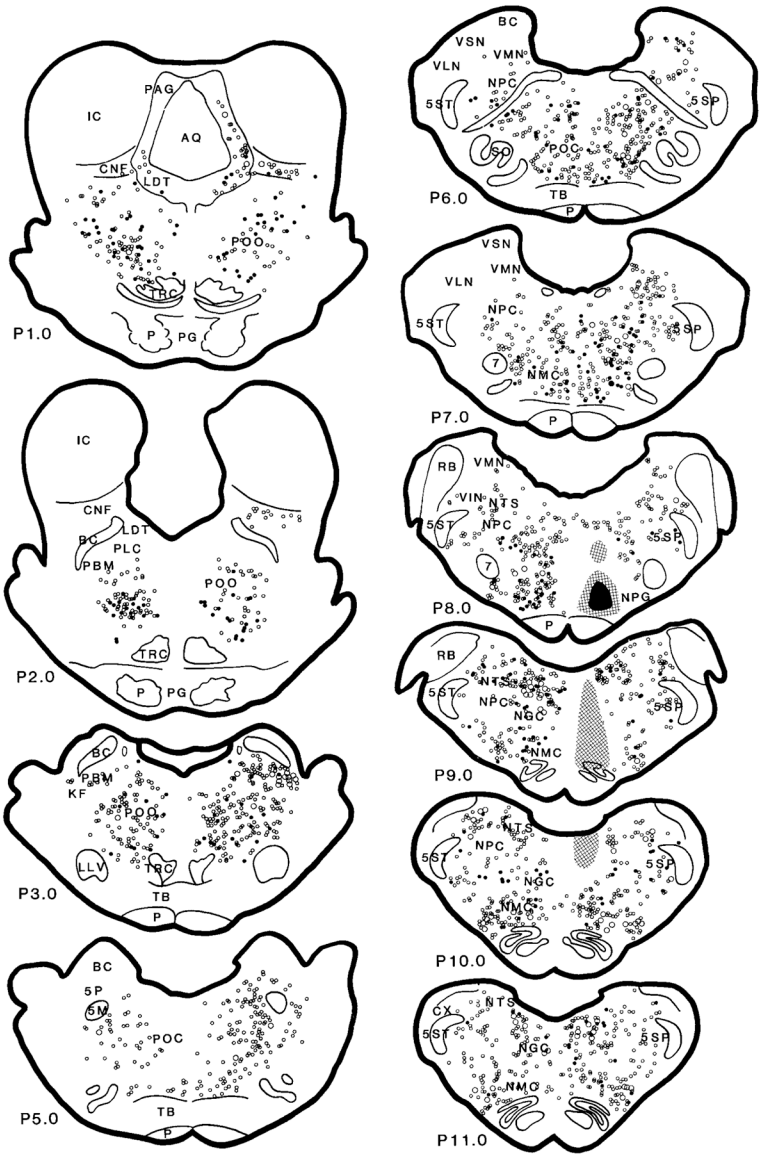

Fig. 6.

Distribution of wheat germ agglutinin–horseradish peroxidase (WGA-HRP; open circles) and WGA-HRP double-labeled with nicotinamide adenine dinucleotide phosphate-diaphorase (filled circles) neurons in the brainstem projecting to the nucleus magnocellularis (case HM11). The small and large symbols represent one and five neurons, respectively. For abbreviations, see list.

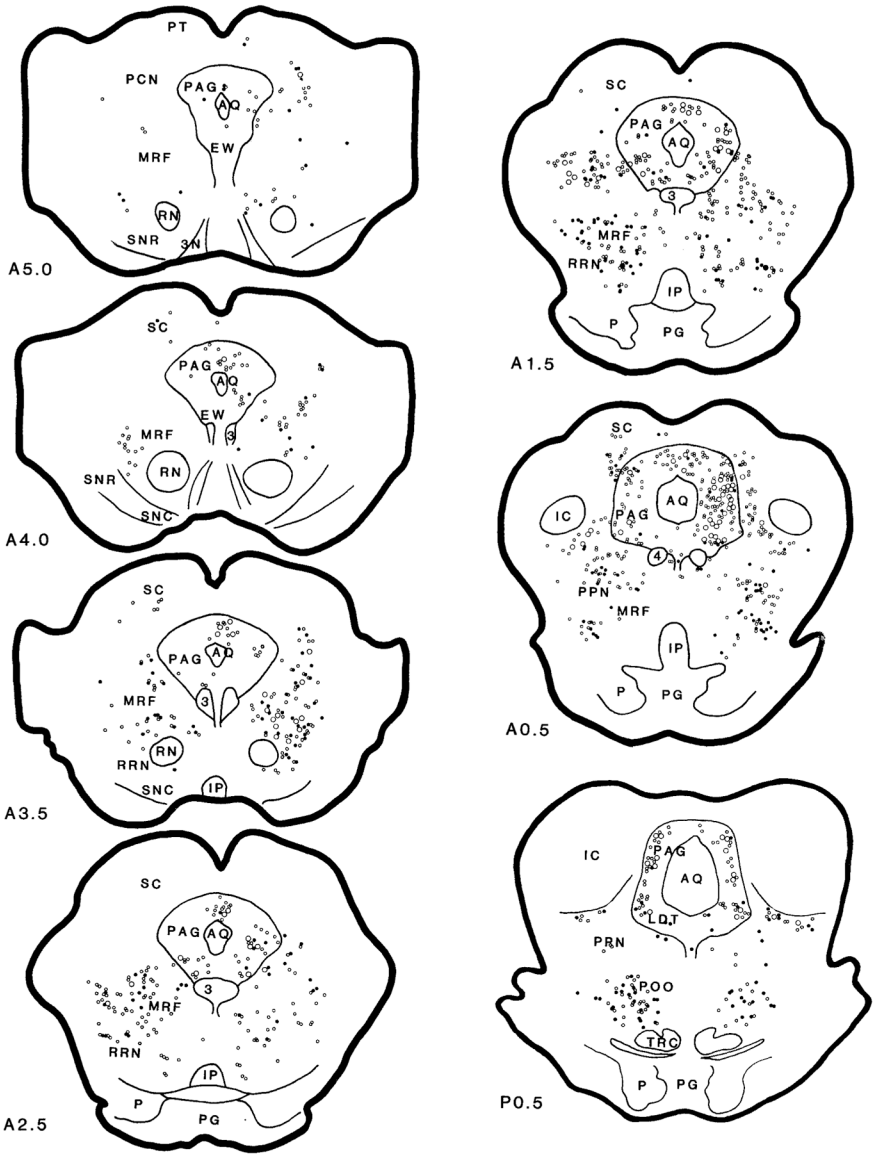

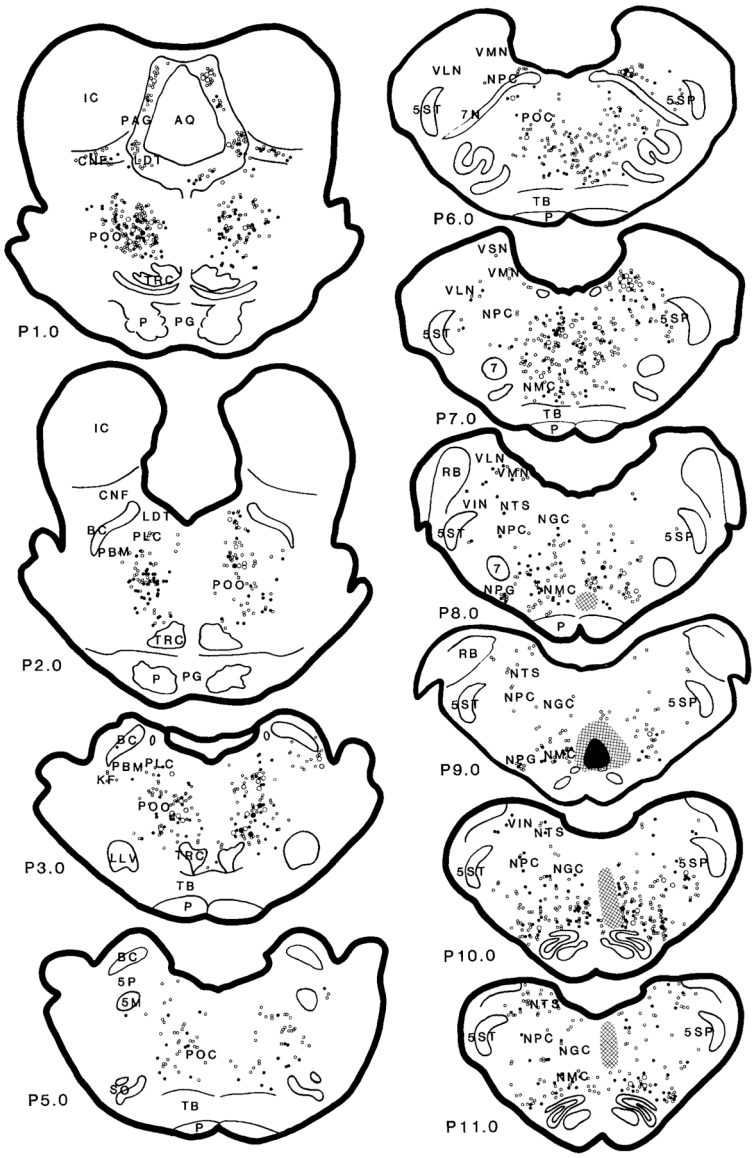

Fig. 7.

Distribution of wheat germ agglutinin–horseradish peroxidase (WGA-HRP; open circles) and WGA-HRP double-labeled with glutamate (filled circles) neurons in the brainstem projecting to the nucleus magnocellularis (case HM22). For abbreviations, see list.

TABLE 1.

Retrogradely Labeled Neurons in the Brainstem Nuclei With Nucleus Magnocellularis WGA-HRP Injections[1]

	Cat[2]					
	HM11/HM13	**HM22**	**HM21**	**HM12**	**HM14**	**HM15**
MRF	++++/++	++/++	+++/+++	+/+	+++/++	+/−
EW	++/+	+/−	+/−	+/+	+/−	−/−
PAG						
Midbrain	+/+	++++/++	++++/++	++/+	+++/++	+/−
Pons	++++/+	+++/+++	++++/+++	+++/+	++++/++	−/−
RRN	+++/++	++/+	+/+	+/−	+++/++	−/−
PPN	+/+	+/+	+/+	+/+	+/+	−/−
LDT	+/+	+/−	+/−	+/−	+/−	−/−
CNF	++/+	+++/++	+++/++	+/+	++/+	−/−
DRN	+/−	+/−	+/−	+/−	+/−	−/−
LC	−/−	−/−	−/−	−/−	−/−	−/−
KF	++++/+	+/−	−/−	++/−	+/−	−/−
PBM	++++/+	+++/+	++/+	+++/+	+++/+	−/−
PoO	++/++++	++/+++	+/+++	++/++++	++/++++	−/−
PoC	++++/+++	++++/+++	++++/+++	++/++	+++/+++	−/−
NPC	++/+	+++/+	+++/+	++/+	++/+	−/−
VSN	+/−	++/+	++/+	+/−	+/−	−/−
VMN	−/+	+/+	+/+	+/+	−/+	−/−
VLN	++/++	++/+	+/+	+/+	++/+	−/−
VIN	++/++	+/+	+/+	+/+	++/+	−/−
5SP	++/+	+/+	+/+	+/+	+/+	−/−
NGC	NA/++	NA/++	NA/+	NA/++	NA/++	NA/+
RVLM	+++/+++	++/+	+++/+	++/+	+++/++	+/−
IO	−/−	NA/++	−/−	NA/+	−/−	−/+

[1] For abbreviations, see list.

[2] Case numbers correspond to the case numbers and injection sites illustrated in Figure 2. Density of ipsilateral/contralateral retrogradely labeled neurons are indicated as follows: −, no retrograde labeling; +, 1–10; ++, 11–20; +++, 21–35; and ++++, ≥36 neurons; NA, data not available due to needle penetration.

TABLE 2.

Percentage of Double-Labeled Glutamate/WGA-HRP (G/H) and NADPH-d/WGA-HRP (N/H) in WGA-HRP-Labeled Neurons[1]

	HM11		HM22		HM21		HM12	
	G/H	N/H	G/H	N/H	G/H	N/H	G/H	N/H
MRF	58	19	22	13	25	25	25	14
RRN	55	29	50	11	38	57	0	25
PAG	24	4	1	2	15	0	14	2
PoO	51	30	35	14	41	12	46	10
PoC	35	8	31	7	46	3	46	10
LDT	25	14	14	0	13	0	24	0
PPN	52	4	39	0	48	0	34	7
CNF	15	6	33	0	15	0	4	10
KF/PBM	21	0	0	0	16	0	33	27
NPC	54	13	32	23	46	11	46	9
VSN	50	27	0	40	57	0	50	57
VLN	47	5	41	24	54	27	27	11
VMN	44	0	19	24	8	23	44	5
VIN	43	7	34	15	29	60	33	0
RVLM	54	6	36	8	32	30	32	0
5SP	65	14	33	38	51	21	5	0
NGC	58	11	42	17	18	32	17	18
NMC	68	35	40	28	33	36	26	9

[1]The percentage of double-labeled neurons of total WGA-HRP-labeled neurons was calculated from both sides of the nuclei, except for the NMC, where data were collected from the side contralateral to the injection. For abbreviations, see list.